The quantification of growth hormone secretion : application of model-informed drug development in acromegaly

Esdonk, M.J. van

Chapter 8

Estimating and simulating endogenous pulsatile growth hormone secretion in healthy controls and acromegaly patients

Authors:

Michiel J. van Esdonk

Jacobus Burggraaf

Ferdinand Roelfsema

Piet H. van der Graaf

Jasper Stevens

Abstract

Endogenous growth hormone (GH) secretion is highly pulsatile and variable between individuals, especially in patients with acromegaly. This study reports on the quantification of this pulsatile GH secretion, by inclusion of a Markovian hypothalamic pulse generator in a model with physiological information on GH stimulation by GH releasing hormone (GHRH), on 24h endogenous GH profiles from healthy controls (n=123) and different cohorts of acromegaly patients (n=56). A pulse identification algorithm was developed to estimate the underlying Markov chain of resting, low and high GHRH secretion states. Cohort specific population parameters were estimated and the transition probabilities between Markov states were quantified. Significant effects of sex and night-time on the occurrence of GHRH secretion states were identified. Close similarity in the 24h mean and area under the curve of observed and simulated endogenous GH profiles was quantified. The developed model can now be used to simulate realistic GH profiles to study the effect of sampling strategies and trial design in acromegaly research.

Keywords

Growth hormone – Pulsatile secretion – Markov model – Growth hormone releasing hormone

Introduction

Growth hormone (GH) secretion is primarily stimulated by the pulsatile release of growth hormone releasing hormone (GHRH), secreted from the arcuate nucleus of the hypothalamus [1]. GHRH is released in the median eminence and travels to the anterior pituitary where it binds to its extracellular receptor on the somatotroph to stimulate GH secretion. However, the timing of the underlying GHRH secretory events and the amount of GHRH released by the hypothalamus is unknown. A deconvolution analysis on endogenous GH profiles may identify these secretory events underlying the data but, due to the empirical nature of this method, lack the capability to incorporate mechanistic information on the biological system [2]. This mechanistic information becomes increasingly important when studying GH secretion in disease states such as acromegaly, in which multiple physiological components are altered, due to the existence of a pituitary adenoma. Also, information after surgical removal of such an adenoma may be helpful to understand (partial) reversal to normal physiology.

The interaction of the stimulatory properties of GHRH on GH secretion have been previously quantified in a population model which included physiological information, in which the GH kinetics and the GHRH stimulatory properties were quantified on data from different experiments in the same individuals (Chapter 7). However, this model did not include a GHRH pulse generator to describe the endogenous pulsatility in GHRH secretion resulting in the characteristic endogenous GH profile. Therefore, this study focused on the expansion of this model with a hypothalamic GHRH pulse generator, modelled as a multi-state discrete time Markov model.

This study reports on the quantification of endogenous pulsatile GH secretion in healthy controls and different groups of acromegaly patients by the inclusion of a hypothalamic pulse generator. Additionally, explanatory variables on the population parameters and the pulse occurrence were explored.

Methods

Data

Data from different sources were combined in order to obtain a large and heterogeneous sample size with endogenous 24h GH profiles, collected at 10 minute intervals. All concentration units were converted using their corresponding conversion factors to mass units (ng/mL). Plasma GH samples from all data sources were measured using the Delfia hGH kit.

Healthy normal weight and obese women

This cohort originated from a study in which the effect of differences in body fat distribution were investigated [3, 4]. In this study, 24 women were included (8 normal weight, 8 lower body obese and 8 upper body obese) and 24h profiles were obtained during the early follicular phase of the menstrual cycle. Obese women returned for a second visit after a weight loss program and repeated the 24h GH profile determination. These data were previously used for the quantification of the individual GH kinetics (Chapter 7).

Healthy men and women

This data originated from different sources in which the healthy men and women participated as placebo or control subjects [5, 6]. The 24h endogenous GH profiles of healthy men (n=41) and women (n=58) with information on their age and body mass index (BMI) was included. During the 24h sampling period, the participants were not allowed to eat snacks, drink beverages with caffeine, exercise or smoke.

Acromegaly patients

Data from different cohorts of acromegaly patients were included in this study. A total of 24 untreated (active) acromegaly patients, 15 patients more or less immediately (short) after transsphenoidal surgery (median = 10 days after surgery) and 17 patients long after transsphenoidal surgery (median = 4.2 years) were studied here [5].

An overview of the subject characteristics from each cohort is presented in Table 1.

Table 1: Subject demographics presenting the median [inter-quartile range] for each available dataset used in this study.

	Healthy normal weight and obese women	**Healthy men and women**	**Acromegaly patients**		
			Active acromegaly	**Short after surgery**	**Long after surgery**
Number of subjects	24	99	24	15	17
Men/Women	0/24	41/58	15/9	6/9	9/8
Age (years)	37 [32.5-41.5]	39 [33.5-48.0]	47.5 [42.8-61.5]	51 [39.5-67.5]	51.5 [44.8-61.5]
Body Mass Index (kg/m^2)	30.3 [25.3-32.1]	27.2 [23.2-32.2]	25.8 [23.7-28.4]	28.1 [26.3-29.3]	29.7 [25.8-31.0]
Available data	Individual GH kinetics + 24h GH profiles	24h GH profiles	24h GH profiles	24h GH profiles	24h GH profiles

Model development

A previously developed non-linear mixed effects (NLME) model for stimulated GH secretion (Chapter 7) incorporated the feed-forward stimulation of GH by GHRH. This model included physiological information on the systemic circulation, the distribution and elimination kinetics of GHRH and GH, and the stimulatory properties of GHRH. In the current study, the pulsatile release of endogenous hypothalamic GHRH was incorporated. The hypothalamic GHRH component was incorporated as a discrete time Markov model (Figure 1) releasing bursts of GHRH in the median eminence when the system was in a secretion state. An additive residual error component was estimated to improve the model fit in the highest concentration regions.

Pulse identification algorithm

A pulse identification iteration algorithm was deployed to estimate the location of the underlying hypothalamic GHRH secretion events in an individual's 24h GH profile. The iteration algorithm started with initializing all states to 0 (resting state) and changing every individual state underlying an individual's GH observation to a secretion state in an iterative procedure. Model improvement was judged on a drop in the Bayesian information criteria (BIC), indicative of the model fit, and successful minimization. The state sequence with the largest improvement in model fit was taken forward in the analysis, and the algorithm was repeated. Pulse identification was completed when the addition of additional pulse locations did not meet the pre-specified drop in BIC.

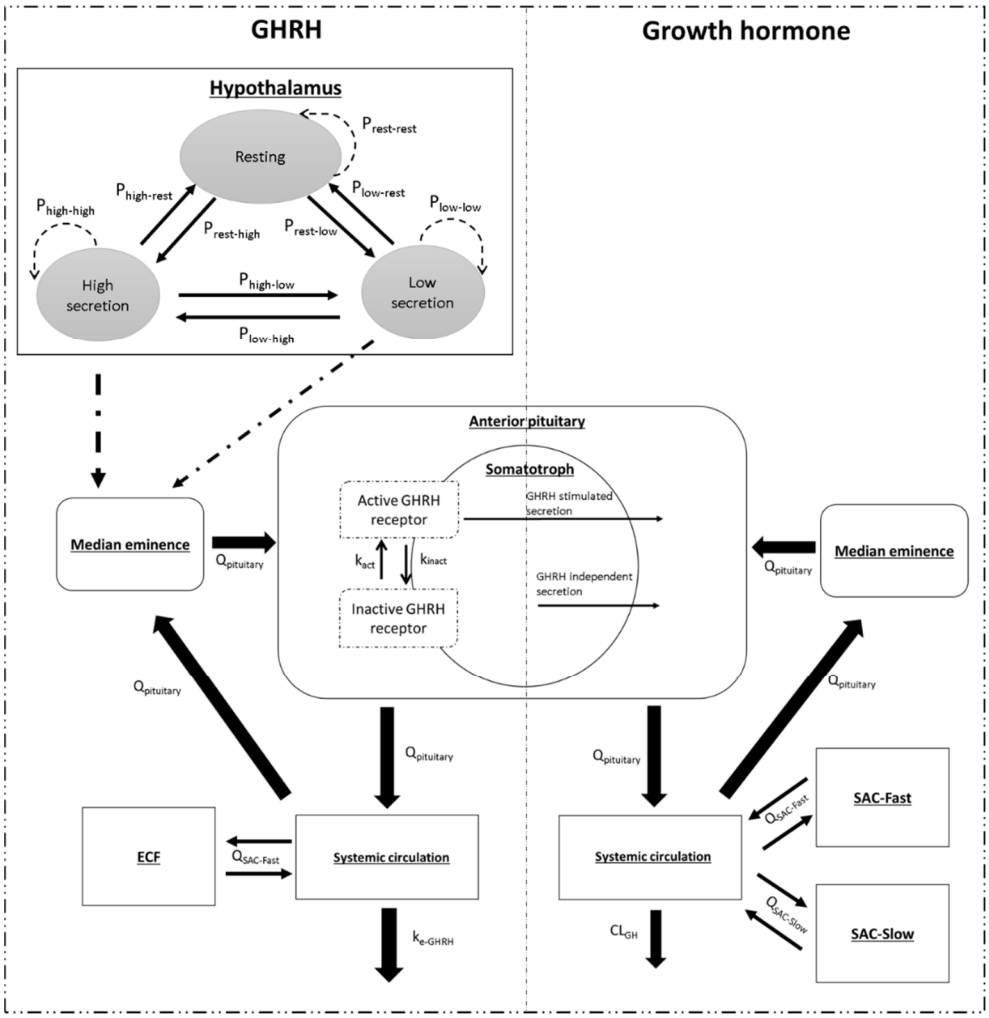

Figure 1: Structural model outline of the growth hormone model with a three-state discrete time Markovian GHRH pulse generator driving GHRH secretion (Hypothalamus, grey). P_{X-Y} = Probability of transitioning from state x to state y.

To reduce the number of possible pulse locations, and thereby improve the algorithm's efficiency, it was investigated whether the use of including secretion events solely at positive delta's with the previous observations would result in equal model predictions (Equation 1).

Equation 1: $x_{\Delta} = x_i - x_{i-1}$

Where x_{Δ} is the difference between the observation at time i (x_i) and the previous (x_{i-1}) observation. An example of these identified positive delta regions in an individual GH profile is depicted in Supplemental material 1.

Feedback identification

The previously developed feed-forward regulation model did not include any feedback components due to the single dose of GHRH administered to subjects (Chapter 7). The improvement in description of endogenous GH profiles by inclusion of a negative feedback component was explored in this study, using the 24h GH profiles from healthy normal weight and obese women as a reference, in which the individual GH kinetics were included. The model used for feedback identification solely included pulses of the same height (creating a two-state discrete time Markov model with a resting and a secretion state) to allow a reduced GH secretion to be the result of the potential feedback component. It was assessed if the observed plasma GH concentrations would, via one or multiple transit compartments, inhibit the secreted GHRH and thereby reduce the pulse amplitude. Additionally, a delay in the feedback was explored in which the observed GH concentration of 30 or 60 minutes earlier was driving the inhibitory response on the GH secretion [7]. A sigmoid maximal effect (E_{MAX}) relationship was tested and judged primarily on an improvement in model fit, the parameter estimates and parameter precision (relative standard errors [RSE]).

Pulse location and transition probabilities identification

The developed algorithm was applied for the estimation of the state sequence in the different cohorts (healthy normal weight and obese controls, patients with active acromegaly, patients short after surgery, patients long after surgery). First, the pulse identification algorithm was run to identify the high secretion states, extracting the highest pulses in a GH concentration-time profile. Afterwards, a second run of the algorithm was performed to add pulses with a low GHRH secretion rate. The rate of the low GHRH secretion state was estimated as a fraction of the high secretion rate.

The improvement of adding an additional secretion state to the Markov model was judged on decreases in the residual error component and visual exploration of the model fit.

The identified state sequence was implemented in a discrete time Markov model for the estimation of the transition probabilities between states. The transition probabilities of transitions which did not occur in the data were fixed to 0.

Covariate exploration

The covariates on which data was available in all subjects (age, BMI, sex) were investigated as explanatory variables of the variability on the parameter estimates of the NLME model and the transition probabilities of the Markov model. In the Markov model, the difference between day- and night-time (10 pm – 6 am) on the $P_{rest\text{-}high}$ and $P_{rest\text{-}low}$, corresponding with the probabilities of going from the resting to a high or low secretion state, were investigated. Covariates were centered around their median values and included in the model following a forward inclusion ($p < 0.01$) with backward elimination method.

Day-to-day variability

No consecutive day-to-day profiles were available in the current dataset to identify day-to-day variability in the population parameters. In order to estimate whether solely the difference in the Markov chain (the pulse locations) could account for the variability between days in the same individual, the ratio between day 1 and day 2 mean GH concentrations was calculated and compared with data from Kraftson *et al*. for the active acromegaly patients [8]. A total of 10.000 48h GH profiles were simulated to quantify the mean ratio and the 95%-confidence interval between day 1 and day 2.

Model evaluation

The exploration of pulse locations were iterated over all sampling time points and judged on the lowering in the BIC, equation 2, and successful model minimization.

Equation 2: BIC = OFV + Number of parameters * log(NOBS)

Where OFV is the objective function value, which equals -2*Log Likelihood, and log(NOBS) is the natural logarithm of the number of observations. To avoid an overly conservative criterion for pulse inclusion in the study's dense data, we used NOBS = 15, which approximates the number of GH observations that might be affected by a single pulse of GHRH (Chapter 7). A $\Delta BIC = -2$ was required for a pulse to be included, in which the inclusion of an extra secretion state was treated as an additional parameter in the model, which corresponds to a minimal drop of 4.7 in the OFV [9]. It should be noted that this drop in OFV is study specific and would change when a different sampling protocol is applied.

The developed model was judged on the individual goodness-of-fit (model predictions versus observations) and the RSE's of the estimated parameters. A total of 10.000 repetitions of Monte Carlo simulations were performed to calculate the 95% confidence intervals in the distribution of the mean and the area under the curve (AUC) of a 24h endogenous GH profile for each population (16h day-time/8h night-time). These simulations included simulated Markov chains, inter-individual variability on the population parameters, and residual error, with sample sizes, sex and BMI distributions corresponding to each population. Additionally, a 24h GH simulation including only the variability in the Markov chain and residual error was performed for 2 subjects per population for illustrative purposes.

Software

NLME modelling was performed in NONMEM V7.3 [10]. Data transformation and visualizations were performed in R version 3.5.1 [11]. Simulations were performed using mrgsolve in R [12].

Results

The use of Equation 1 as a selection criteria to pre-select potential pulse locations resulted in an equal model fit, with decreased runtimes, and was therefore preferred. The inclusion of a feedback component, that could account for changes in the GH pulse amplitudes, driven by the amounts in transit compartments or by a 30 or 60 minute delay, reduced in a decreased description of the data in this study in a majority of individuals (Figure 2). This indicates that no significant impact of a feedback component on the endogenous 24h GH profiles could be identified.

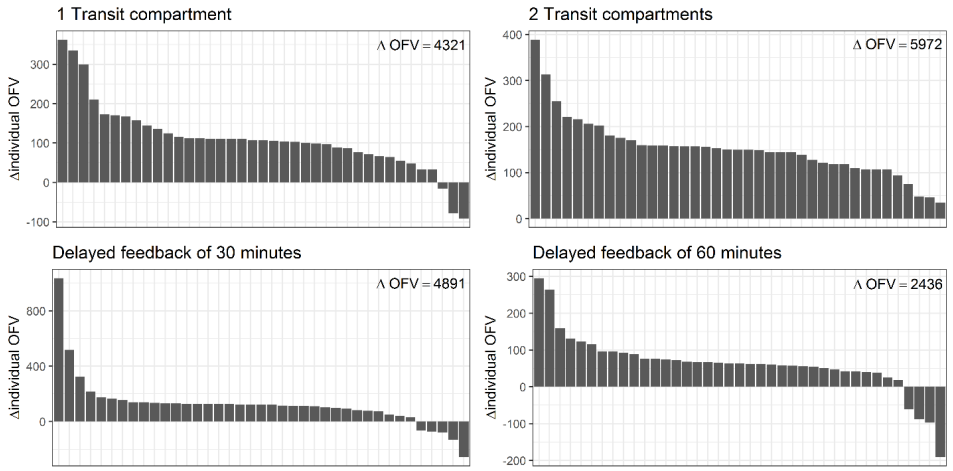

Figure 2: Waterfall chart showing the individual in- or decrease in objective function value (OFV) after inclusion of different feedback mechanisms. ΔOFV presented in the top right corner of each facet is the total change from the reference OFV (no feedback component). Negative ΔOFV indicates an improvement in model fit.

Pulse identification

Healthy controls

The developed iteration algorithm was able to capture the highest GH bursts in a 24h profile by inclusion of solely a high secretion state with an additive residual error, however, resulted in a mis-prediction of the lowest pulses (Supplemental material 2A). The addition of a supplementary low secretion state significantly improved the model fit, due to the additional freedom of the model to account for a lower pulse secretion rate (Supplemental material 2B). This inclusion reduced the additive residual error (σ^2) from 0.28 to 0.11. The addition of another lower secretion state, creating a four-state Markov model, was not explored due to the low level of remaining residual error and adequate individual description of the data. Inclusion of the previously identified covariate relationship of bodyweight on GH clearance gave a significant improvement in the model fit ($p < 0.01$) (Chapter 7).

No other covariate relationships on the population parameters were identified. The estimated model parameters are given in Table 2 and all parameters were estimated with low RSE's. The pituitary activity was fixed to 100% to serve as a reference for the patient populations.

The individual model predictions closely followed the line of unity, especially in the highest concentration regions (Supplemental material 3). No bias over the time of day or over the population predictions was identified.

Table 2: Model parameter estimates (% RSE) [% shrinkage] presented for each cohort.

	Healthy controls	**Active acromegaly**	**Short after surgery**	**Long after surgery**
		Population parameters		
k_{inact} (/h)	2.63 (2.83)	2.63 [a]	2.63 [a]	2.63 [a]
Pituitary activity	100%[a]	315% (11.3)	59.6 % (16.5)	59.7% (13.1)
High secretion rate (nmol GHRH/h)	0.0986 (5.0)	0.0986 [a]	0.0986 [a]	0.0986 [a]
Low secretion rate (% of high secretion rate)	36.4 (3.8)	49.8 (16.2)	26.5 (13.8)	34.1 (6.83)
GHRH independent secretion (μg/h)	2.93 (5.0)	310 (10.9)	9.2 (18.8)	3.9 (14.8)
		Inter-individual variability		
ω^2 k_{inact}	0.109 (13.58) [4.4]	-	-	-
ω^2 Pituitary activity	-	0.748 (32) [1.8]	0.411 (37.7) [<0.01]	0.389 (38.8) [<0.01]
ω^2 High secretion rate	0.494 (12.83) [3.5]	-	-	-
ω^2 Low secretion rate	0.134 (16.0) [14.4]	0.247 (67) [39.2]	0.196 (55) [17.8]	0.077 (42) [18.6]
ω^2 GHRH independent secretion	0.46 (15.2) [16.2]	0.893 (30) [<0.01]	0.536 (40.6) [<0.01]	0.33 (40) [4.8]
		Residual error		
σ^2 Additive error	0.106 (1.02) [1.2]	17 (2.4) [0.8]	0.0545 (3.0) [0.9]	0.0479 (2.9) [0.85]

[a] *= fixed parameter.*

Acromegaly patients

In acromegaly patients, the estimated k_{inact} (2.63/h) and high GHRH secretion rate (0.0986 nmol GHRH/h) were fixed to the parameter estimates of healthy controls since no biological difference in this value was assumed between cohorts. The pituitary activity was estimated as a separate parameter to allow for differences in pulse amplitudes between healthy controls and acromegaly patients in the state sequence analysis. The estimation of the patient population specific parameters shows a 215% increase in this activity in active acromegaly patients compared to healthy controls, which was reduced to values lower than the healthy controls both shortly (59.6%) or long (59.7%) after surgery (Table 2). In active acromegaly patients, the low secretion rate was 49.8% of the high secretion rate, which was higher compared to the other cohorts. A more than 100-fold increase, compared to healthy controls, in the GHRH independent (basal) GH secretion was estimated in active acromegaly patients compared to healthy controls. These results indicate that active acromegaly patients have higher bursts of GH and higher continuous basal GH secretion.

The parameter estimates for each individual cohort are presented in Table 2. All parameters were estimated with low RSE's (<20%), indicating high parameter precision. However, high η-shrinkage on the low secretion rate was identified (39.2%). An omega block was included for the active acromegaly cohort between the GHRH independent secretion and the pituitary activity, identified by correlation plots (estimated correlation 0.727). A wide scatter around the line of unity of the population predictions was identified (Supplemental material 4), especially in the active acromegaly patients. This was adequately captured in the individual model predictions which are closely distributed around the line of unity in all populations. No bias in the predictions over time of day or over the population predictions was identified. These results indicate that the current model is able to describe endogenous GH secretion across all cohorts, while accounting for the variability in pulsatile GH secretion.

Transition probabilities

The estimated Markov transition probabilities are given in Table 3 and the estimated covariate parameters in Table 4. In the Markov analysis of the state sequence in healthy controls, a significant sex effect of -33.4% in men on both probabilities originating from the resting state ($P_{rest\text{-}high}$ & $P_{rest\text{-}low}$) was identified. A clear influence of night-time on the occurrence of the high secretion state was identified, resulting in an 88.3% higher probability of the occurrence of this high secretion state during the night in healthy controls. In active acromegaly patients, the $P_{rest\text{-}high}$ was more than doubled (from 2% to 5%) compared to healthy controls, indicating more high secretion events in this population. The influence of night-time on GH secretion remained visible in this cohort of patients ($P_{rest\text{-}high}$ = +76% during the night) whereas the previously identified sex difference from healthy controls was not significant. There was a reduction in all other probabilities compared to healthy individuals, suggesting an increase in high pulses and a reduction in low pulses in active acromegaly patients.

Table 3: Markov transition matrix with estimated transition probabilities (% relative standard error).

	From:	**To:**		
Healthy controls		***Rest***	***Low***	***High***
	Rest	1 - $P_{rest\text{-}low}$ - $P_{rest\text{-}high}$	0.0299* (1+*SEX_effect**SEX) (5.68%)	0.0188* (1+*SEX_effect**SEX) * (1+ *Night_effect_H**NIGHT) (7.71%)
	Low	1 - $P_{low\text{-}low}$ - $P_{low\text{-}high}$	0.0806 (16.7%)	0.118 (10.7%)
	High	1 - $P_{high\text{-}high}$ - $P_{high\text{-}low}$	0.162 (10.5%)	0.226 (6.21%)
Active acromegaly	***Rest***	1 - $P_{rest\text{-}low}$ - $P_{rest\text{-}high}$	0.0166 (28.12%)	0.053* (1+ *Night_effect_A**NIGHT) (14.59%)
	Low	1 [a]	0 [a]	0 [a]
	High	1 - $P_{high\text{-}high}$ - $P_{high\text{-}low}$	0.0178 (44.71%)	0.0622 (28.41%)
Short/long after surgery	***Rest***	1 - $P_{rest\text{-}low}$ - $P_{rest\text{-}high}$	0.0485* (1+*Long_effect_low**POP) (22.39%)	0.0273* (1+*Long_effect_high**POP) * (1+ *Night_effect_SL**NIGHT) (27.53%)
	Low	1 - $P_{low\text{-}low}$ - $P_{low\text{-}high}$	0.0511 (26.34%)	0.119 (16.34%)
	High	1 - $P_{high\text{-}high}$ - $P_{high\text{-}low}$	0.0607 (31.62%)	0.171 (17.98%)

Women SEX = 0, men SEX = 1; 10 pm – 6 am NIGHT = 1, else NIGHT = 0; short after surgery POP = 0, long after surgery POP= 1; [a] = *fixed parameter*

Table 4: Covariate parameter estimates.

Parameter	**Estimate (% RSE)**
SEX_effect	-0.334 (19.2%)
Night_effect_H	0.883 (22%)
Night_effect_A	0.756 (48.2%)
Long_effect_low	-0.451 (31.22%)
Long_effect_high	-0.551 (26.87%)
Night_effect_SL	1.94 (21.46%)

Due to the similarity of the cohorts shortly or long after surgery and the limited sample size, these cohorts were combined and differences between these two cohorts were tested based on significance. The long after surgery cohort showed to have significantly lower $P_{rest\text{-}low}$ and $P_{rest\text{-}high}$ compared to the short after surgery cohort ($p < 0.05$), however both remained close to the healthy control estimates. A much stronger night-time effect on the $P_{rest\text{-}high}$ was identified in these cohorts (+194%). As in the active acromegaly patients cohort, no sex differences in GH secretion could be identified. All other transition probabilities were similar to healthy controls. These results indicate that both cohorts have similar GH secretion patterns compared to healthy controls, with higher night-time influences.

Internal validation and day-to-day variability

Simulations including the cohort specific parameters with variability and transition probabilities resulted in the correct description of the median distribution of the mean GH secretion and description of the 24h GH area under the curve, with majority of values within the 95% confidence intervals (Table 5). The lower 25% distribution of the data in healthy controls was overpredicted with this model, most likely due to the level of residual error in this healthy control model in this lowest concentration range. All other distributions of all cohorts were well within the confidence interval. The day-to-day variability in the active acromegaly cohort closely resembled data by Kraftson *et al.* [8] (mean ratio = 1.02, 95%-CI = 0.78 – 1.38), indicative that this variability can be solely explained by differences in the pulsatile pattern between days. Simulated endogenous GH profiles of each population resembled endogenous GH secretion in terms of pulse occurrence, pulse height, and basal secretion. The simulated endogenous GH profiles of 2 individuals per cohort are given for illustrative purposes in Figure 3.

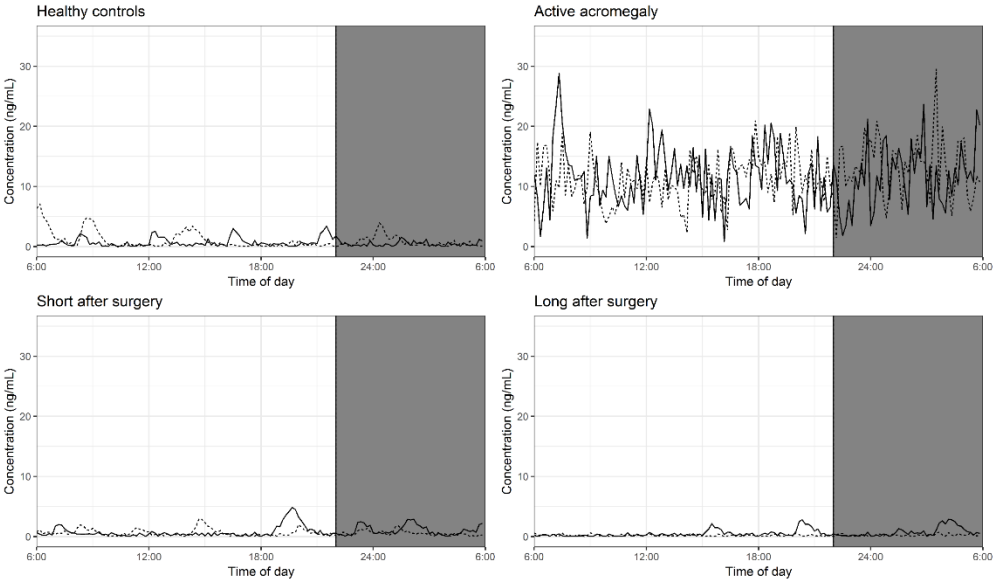

Figure 3: Simulated 24h endogenous GH profiles (1 men and 1 women) per population during day and night (grey).

Table 4: Comparison of observed and simulated distribution of the mean and 24h area under the curve. 95% confidence interval (CI) calculated based on 10.000 simulations of each cohort.

	Mean GH (ng/mL)					
	25th percentile		**50th percentile**		***75th percentile***	
	Observed	***Simulated 95%-CI***	***Observed***	***Simulated 95%-CI***	***Observed***	***Simulated 95%-CI***
Healthy controls	0.32	0.35-0.43[a]	0.55	0.5-0.64	0.94	0.76-1.07
Active acromegaly	7.82	6.44-12.58	18.35	9.65-20.17	30.93	15.21-36.17
Short after surgery	0.55	0.41-0.79	0.67	0.56-1.11	0.90	0.78-1.62
Long after surgery	0.30	0.23-0.36	0.37	0.28-0.49	0.51	0.36-0.71
	Area under the curve in 24h (ng*h/mL)					
	25th percentile		**50th percentile**		**75th percentile**	
	Observed	***Simulated 95%-CI***	***Observed***	***Simulated 95%-CI***	***Observed***	***Simulated 95%-CI***
Healthy controls	7.4	8.4-10.4[a]	13.3	11.8-15.4	22.3	18.1-25.5
Active acromegaly	188.1	153.7-300.6	440.0	230.5-481.9	743.6	363.5-864.8
Short after surgery	13.1	9.9-18.9	16.1	13.4-26.4	21.5	18.6-38.6
Long after surgery	7.1	5.5-8.6	8.8	6.8-11.7	12.3	8.7-16.9

[a] *= 95%-confidence interval outside observed value.*

Discussion

The developed model quantified the endogenous pulsatility in GH secretion in different cohorts, ranging from healthy controls to acromegaly patients before and after surgery. Using a three-state discrete time Markov model, mimicking the hypothalamic GHRH pulse generating function, an adequate description of the data was obtained with high parameter precision in the population parameters. The impact of sex and night-time on the occurrence of GH pulses in the different cohorts was quantified which closely corresponds with biological knowledge. The similarity of the observed mean and area under the curve of 24h endogenous GH profiles shows that the current model is able to simulate realistic cohort specific GH profiles, by the inclusion of the physiological components and inter-individual variability on the parameters.

Hartman *et al.* [13, 14] postulated that the increase in GH secretion in active acromegaly patients mainly originated from basal and not from pulsatile release. This is primarily caused by the 100-fold increase in GHRH independent secretion estimated in this study, resulting in higher basal levels of GH. However, active acromegaly patients did also show to have increased pulse amplitudes and pulse occurrences but this contributed less to the total GH secretion compared to healthy controls. Cohort specific parameter estimates and transition probabilities were quantified in the developed model. The parameters returned to values close to healthy in acromegaly patients after surgery, with similar transition probabilities and lower pituitary activity, indicative of lower pulse amplitudes in the cohorts after surgery.

Multiple significant covariates impacting the occurrence of GH pulses have been identified. Increased GH release during the night is a common biological phenomenon which was confirmed in all cohorts by at least an 76% increase in probabilities going towards a high secretion state during the night [15, 16]. The sex related differences identified in the healthy controls cohort resulted in a less stochastic GH profile in men, due to the decrease in $P_{rest\text{-}high}$, which is in agreement with literature [17, 18]. The sex related differences were not identified in the acromegaly cohorts. The GH secreting properties of a pituitary adenoma, and the high level of variability in these populations, with a lower sample size compared to the healthy controls cohort, were most likely to cause this discrepancy. Furthermore, it was expected that a significant effect of age would be identified, however, this could not be identified in the current dataset [19, 20].

The implementation of delayed differential equations, with a 30 minute or 60 minute delay, focused on the existence of a long feedback loop in the system as was implemented by MacGregor *et al.* [7]. Although such feedback mechanism is described in various literature sources [21, 22], the inclusion of this delayed feedback worsened the fit of the data, which indicates that no relationship could be identified between a previous GH pulses and a subsequent pulse height. Another feedback component in the GH system is the short feedback loop, which causes a fast inhibitory response after a GHRH pulse, inhibiting further GHRH and GH secretion. This loop was captured by the high $P_{high\text{-}rest}$ ($P>0.6$) in all

cohorts, which causes the hypothalamus to have a quick transition from a high secretion state back to a resting state, possibly caused by GH itself or somatostatin, but was not defined as such due to the lack of data on local hormone concentrations.

The implementation of a Markov model as a pulse generator remains to be an empirical component [23], however, is required when the stimulatory factors of a system are not available. For example, stress, glucose, hunger, and activity levels of an individual could all explain part of the occurrence of transitioning to a secretion state but were currently unknown. Therefore, the included Markov model contains information that could be stratified into physiological stimulatory pathways in the future when additional data becomes available. Especially the inclusion of the ghrelin concentrations and its stimulatory properties could improve the mechanistic description of this axis, since the current model assumes GH stimulation solely by GHRH [24].

Summarizing, the developed model is able to simulate the 24h mean and area under the curve of GH profiles in all different cohorts, indicating that this model can be used to study GH kinetics, GHRH driven GH secretion, and endogenous pulsatile GH secretion. The model including the hypothalamic GHRH pulse generator can be used for the quantification of drug effects, for clinical trial simulations, and to identify which simplified sampling protocol best represents actual GH secretion, all while including the cohort specific parameters and the variability in endogenous GH secretion.

Acknowledgments

We thank S.C. Goulooze for his help in discussing the BIC cut-off criteria for pulse selection and the development of the discrete time Markov models.

References

1. Frohman LA, Downs TR, Clarke IJ, Thomas GB (1990) Measurement of growth hormone-releasing hormone and somatostatin in hypothalamic-portal plasma of unanesthetized sheep. Spontaneous secretion and response to insulin-induced hypoglycemia. J Clin Invest 86:17–24.
2. Johnson ML, Pipes L, Veldhuis PP, Farhy LS, Boyd DG, Evans WS (2008) AutoDecon, a deconvolution algorithm for identification and characterization of luteinizing hormone secretory bursts: description and validation using synthetic data. Anal Biochem 381:8–17.
3. Langendonk J, Veldhuis J, Burggraaf J, Schoemaker R, Cohen A, Meinders E, Pijl H (2001) Estimation of growth hormone secretion rate: impact of kinetic assumptions intrinsic to the analytical approach. Am J Physiol Regul Integr Comp Physiol 280:225–232.
4. Pijl H, Langendonk JG, Burggraaf J, Frölich M, Cohen AF, Veldhuis JD, Meinders AE (2001) Altered neuroregulation of GH secretion in viscerally obese premenopausal women. J Clin Endocrinol Metab 86:5509–5515.
5. Roelfsema F, Biermasz NR, Pereira AM, Veldhuis JD (2016) Optimizing blood sampling protocols in patients with acromegaly for the estimation of growth hormone secretion. J Clin Endocrinol Metab 101:2675–82.
6. Roelfsema F, Veldhuis JD (2016) Growth Hormone Dynamics in Healthy Adults Are Related to Age and Sex and Strongly Dependent on Body Mass Index. Neuroendocrinology 103:335–344.
7. MacGregor DJ, Leng G (2005) Modelling the hypothalamic control of growth hormone secretion. J Neuroendocrinol 17:788–803.
8. Kraftson A, Barkan A (2010) Quantification of day-to-day variability in growth hormone levels in acromegaly. Pituitary 13:351–354.
9. Raftery AE (1995) Bayesian Model Selection in Social Research.
10. NONMEM version 7.3.0 (Beal, S., Sheiner, L.B., Boeckmann, A., & Bauer, R.J., NONMEM User's Guides. (1989-2013), Icon Development Solutions, Ellicott City, MD, USA, 2013).
11. R Core Team (2018). R: A language and environment for statistical computing. R Foundation for Statistical Computing, Vienna, Austria. URL https://www.R-project.org/.
12. Baron KT, Gastonguay MR (2015) Simulation from ODE-Based Population PK/PD and Systems Pharmacology Models in R with mrgsolve. J Pharmacokinet Pharmacodyn 42:S84–S85.
13. Hartman ML, Veldhuis JD, Vance ML, Faria ACS, Furlanetto RW, Thorner MO (1990) Somatotropin pulse frequency and basal concentrations are increased in acromegaly and are reduced by successful therapy. J Clin Endocrinol Metab 70:1375–1384.
14. Hartman ML, Pincus SM, Johnson ML, Matthews DH, Faunt LM, Vance ML, Thorner MO, Veldhuis JD (1994) Enhanced basal and disorderly growth hormone secretion distinguish acromegalic from normal pulsatile growth hormone release. J Clin Invest 94:1277–1288.
15. Brandenberger G, Weibel L (2004) The 24-h growth hormone rhythm in men: sleep and circadian influences questioned. J Sleep Res 251–255.
16. Van Cauter E, Plat L (1996) Physiology of growth hormone secretion during sleep. J Pediatr 128:S32-7.
17. Hindmarsh PC, Dennison E, Pincus SM, Cooper C, Fall CHD, Matthews DR, Pringle PJ, Brook CGD (1999) A Sexually Dimorphic Pattern of Growth Hormone Secretion in the Elderly. J Clin Endocrinol Metab 84:2679–2685.
18. Van Den Berg G, Veldhuis JD, Frölich M, Roelfsema F (1996) An amplitude-specific divergence in the pulsatile mode of growth hormone (GH) secretion underlies the gender difference in mean GH concentrations in men and premenopausal women. J Clin Endocrinol Metab 81:2460–2467.
19. Hersch EC, Merriam GR (2008) Growth hormone (GH)-releasing hormone and GH secretagogues in normal aging: Fountain of Youth or Pool of Tantalus? Clin Interv Aging 3:121–9.
20. Chertman LS, Merriam GR, Kargi AY (2000) Growth Hormone in Aging. Endotext
21. Tannenbaum GS, Painson JC, Lapointe M, Gurd W, McCarthy GF (1990) Interplay of somatostatin and growth hormone-releasing hormone in genesis of episodic growth hormone secretion. Metabolism 39:35–39.
22. Gunawardane K, Krarup Hansen T, Sandahl Christiansen J, Lunde Jorgensen JO (2000) Normal Physiology of Growth Hormone in Adults. MDText.com, Inc.
23. Danhof M (2016) Systems pharmacology – Towards the modeling of network interactions. Eur J Pharm Sci 94:4–14.
24. Roelfsema F, Biermasz NR, Veldman RG, Veldhuis JD, Frölich M, Henriëtte Stokvis-Brantsma W, Wit JM (2001) Growth hormone (GH) secretion in patients with an inactivating defect of the GH-releasing hormone (GHRH) receptor is pulsatile: Evidence for a role for non-GHRH inputs into the generation of GH pulses. J Clin Endocrinol Metab 86:2459–2464.

Supplemental materials

1. Pre-specified pulse locations

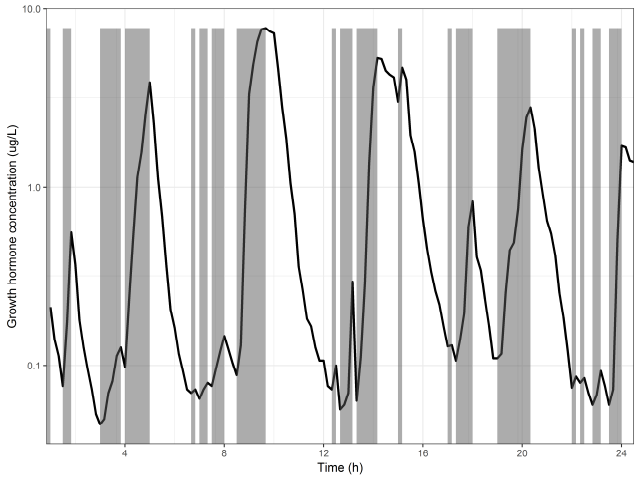

Example 24h GH profile with the selected positive delta regions (grey) on which an increase in the concentration was identified. A change in state sequence was explored in only these regions.

2. Addition of a low secretion state on model fit

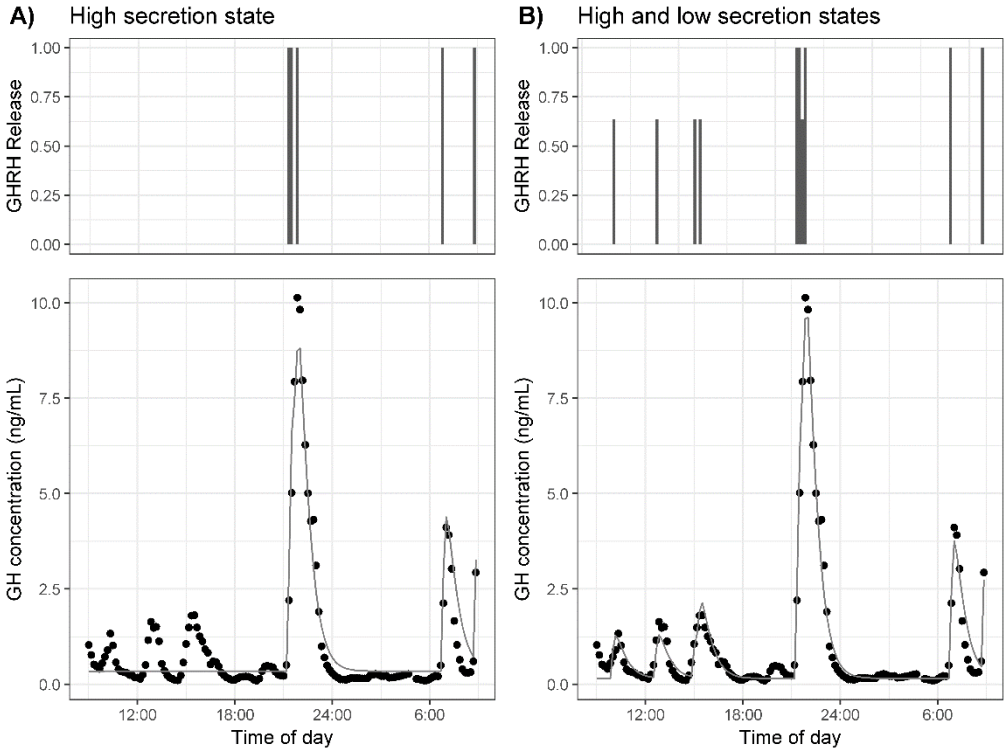

Model fit using a high secretion state only (A) or a high and low secretion state (B). Top: predicted growth hormone releasing hormone (GHRH) release, Bottom: observations (circles) with individual model predictions over time of day (line). GHRH release represents the high or low secretion states of the hypothalamus.

3. Goodness-of-fit plots healthy controls

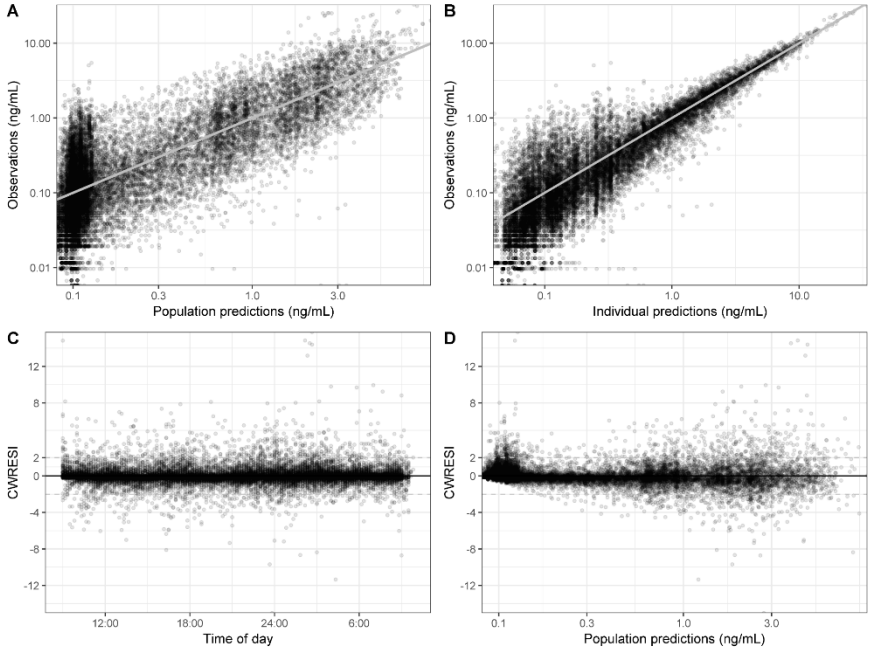

A) Population model predictions versus observations, B) individual model predictions versus observations, C) CWRESI versus time of day, D) conditional weighted residuals with interaction (CWRESI) versus population predictions. Black diagonal line = line of unity, grey dashed line = [-2, 2] interval.

4. Goodness-of-fit plots acromegaly patients

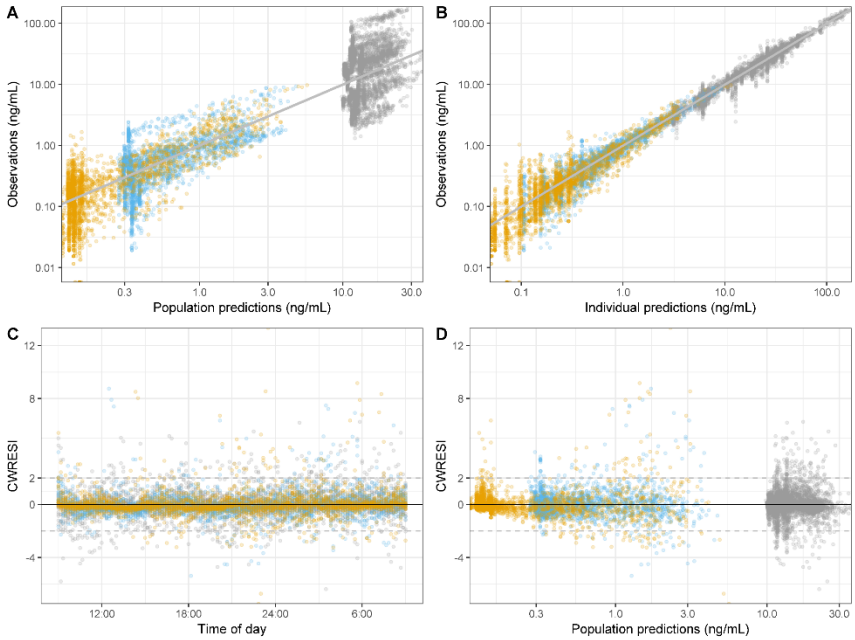

A) Population model predictions versus observations, B) individual model predictions versus observations, C) CWRESI versus time of day, D) conditional weighted residuals with interaction (CWRESI) versus population predictions. Black diagonal line = line of unity, grey dashed line = [-2, 2] interval. Grey = active acromegaly, blue = short after surgery, yellow = long after surgery